International Journal of Advanced Technology and Engineering Exploration, Vol 7(66)
ISSN (Print): 2394-5443 ISSN (Online): 2394-7454
http://dx.doi.org/10.19101/IJATEE.2020.762040

Research Article

The effectiveness method (ε-NTU) to analyze the thermal performance of the flat tube multi-louvered finned radiator with silver nanoparticles suspension in ethylene Glycol

Élcio Nogueira*
Department of Mechanics and Energy - State University of Rio de Janeiro - FAT / UERJ, Brazil

Received: 22-March-2020; Revised: 15-May-2020; Accepted: 20-May-2020

Abstract
The analytical efficacy method (ε-NTU) is applied to analyze the thermal performance of the radiator with Multi-Louvered flat-tube fins. The nanofluid is composed of a suspension of silver nanoparticles in ethylene glycol. The rate of heat transfer, efficiency, and outlet temperatures of the nanofluid and air are determined and presented in graphical form. The volumetric fraction of the nanoparticles suspended in ethylene glycol, the variations in the airflow rate and the nanofluid flow rate is the main parameters used in the analysis. The analysis showed promising results since it is possible to save on the use of the compact heat exchanger considered, reducing costs and storage space for the refrigerant.

Keywords
Effectiveness method, Nanofluid, Multi-louvered finned radiator, Silver nanoparticles, Ethylene glycol, Compact heat transfer.

1.Introduction
The objective of the work is to apply the analytical method of the effectiveness to analyze the thermal performance of the flat tube multi-louvered finned automotive radiator with silver nanoparticles suspension in ethylene glycol.

All internal combustion engines produce heat and friction. This heat can have catastrophic effects on engine components. The existing methods employed to study and minimized this kind of combustion problem are analytical, experimental, and computational methods. The automotive radiator performance can be determined using the analytical method of effectiveness (ε-NTU) [1].

Sany et al. [2] carried out analytical and experimental work to obtain the Nusselt number and heat transfer coefficient. The effectiveness coefficient and the heat transfer coefficient are determined considering experimental data. The same procedures estimate the pressure drop and the Colburn factor for the radiator. Application examples demonstrated the utility of the method used.

Properly dispersed nanoparticles provide an increase in the heat transfer surface between particles because nanofluids have a high specific surface area and high dispersion stability, with a predominant Brownian motion. Besides this, the use of extended surfaces for improving the efficiency of heat transfer is more effective, adding small solid particles to that fluid [3]. Jing et al. [4] developed a new type of air-water heat exchanger to reduce the consumption of energy. The thermal performance and energy efficiency were analyzed and studied using the effectiveness number of transfer units (ε -NTU) method. The main conclusions obtained by the analysis are the air flow rate had a more considerable influence on the performance than the water flow rate and that the maximum heat transfer efficiency was 81.4% with Cmin/Cmax equal 0.25.

Blecich et al. [5] presented a new method for fin-and-tube heat exchangers operating with non-uniform airflow, which consists of discretizing the heat exchanger into tube elements. The results are compared against experimental data. They demonstrated that airflow nonuniformity causes effectiveness deterioration. The effectiveness deterioration depends on the number of heat transfer units (NTU) and the heat capacity rate ratio.

*Author for correspondence

Hussein et al. [6] mention that the main reason for using solid particles smaller than 100 nm is to improve thermal properties. Refrigeration systems and numerous industrial applications often use metallic solids dispersed in water and ethylene glycol. This type of fluid is commonly defined as a nanofluid.

According to Kim and Cho [7], a newly developed louver fin is introducing, and the louver fin has downstream a drainage 3.2 mm width. The new fins were investigated, and the results are compared with those of the sample made of conventional fins. The superior wet surface heat transfer and pressure drop were obtained. The Colbourn factors were 40% larger, and the friction factor was 9% smaller.

Pankaj et al. [8] propose an analytical radiator having a rectangular tube with louvered fins using the effectiveness-NTU method. The procedure is validated with experimental results, and it is found that the maximum deviation in the heat transfer is 10.97, and in pressure drop is about 3.29%.

Numerical analysis and experimental study are applied to determine the performance of an automotive radiator using louvered fin. Reynolds number and radiator boundary conditions were investigated at a louvered angle of 25º. The results indicated an improvement in the Nusselt number and a decrease in the specific fuel consumption when compared to flat-fin geometry at the same operating conditions Gomaa [9].

High-efficiency demand is a capital feature in the automotive radiator, and optimizing the design of an automotive radiator is obtained by the technological development in automotive industries. The design of a louvered fin based compact automotive heater is getting a high cooling rate with nanofluids [10, 11].

Multi-Louvered fins have been studied by experimental methods, analytical methods, and numerical simulations, because of the excellent thermal-hydraulic performance [12, 13].

Junior and Nogueira [14] present research considering silver nanoparticles in a flat tube finned radiator heat exchanger. They demonstrate that the rate of heat transfer can be higher than the use of ethylene glycol and water, or pure water, for relatively low airflow, and that the viscosity of the nanofluid cooling increases with the addition of the volumetric fraction. Besides, they conclude that kinematic viscosity and diffusivity, are significantly higher for nanofluids Nogueira [15].

2.Methodology

Table 1 presents some parameters for the Multi-Louvered finned radiator. Dong et al. [10] obtained the correlations for the J_{Lp}, Colburn factor. These correlations are essential to get the Colburn factor and to apply in theoretical works [11].

In this work, we used, for numerical and graphic determination of the physical quantities of interest, the geometric characteristics presented in *Table 1* and thermal physical properties in *Table 2*.

The radiator is mounted on a turbocharged diesel engine. It consists of 644 tubes manufactured in brass and 346 continuous fins in aluminum alloy whose thermal conductivity is 177 W/(m K).

The numerical correlations used for determination of j factor and f factor are:

$$j_{Lp} = 0.2712 Re_{Lp}^{-0.1944} \left(\frac{L_a}{90}\right)^{0.257} \left(\frac{F_p}{L_p}\right)^{-0.5177} \left(\frac{F_h}{L_p}\right)^{-1.9045} \left(\frac{L_h}{L_p}\right)^{1.7159} \left(\frac{L_d}{L_p}\right)^{-0.2147} \left(\frac{\delta}{L_p}\right)^{-0.05} \quad (1)$$

and

$$Re_{Lp} = \frac{uL_p}{\vartheta} \quad (2)$$

u - air velocity among fins (m/s)
ϑ - viscosity (m^2/s).

The properties of the ethylene-based solution are obtained by the expressions below:

$$\rho_{solution} = \rho_{EG\%} V + (1 - V)\rho_w \quad (3)$$
$$\mu_{solution} = \mu_{EG\%} V + (1 - V)\mu_W \quad (4)$$
$$Cp_{solution} = Cp_{EG\%} V + (1 - V)Cp_w \quad (5)$$
$$k_{solution} = k_{EG\%} V + (1 - V)K_w \quad (6)$$
$$\alpha_{solution} = \frac{k_{solution}}{\rho_{solution} Cp_{solution}} \quad (7)$$
$$\vartheta_{solution} = \frac{\mu_{solution}}{\rho_{solution}} \quad (8)$$
$$Pr_{solution} = \frac{\alpha_{solution}}{\vartheta_{solution}} \quad (9)$$

where V and Eg% are the volume fraction percent of water and weight fraction percent of Ethylene Glycol, respectively. In this work, we are using V=1.0, i.e., the base fluid is pure ethylene glycol. For silver nanoparticles suspension properties, we have:

$$\rho_{nano} = \emptyset\rho_{particle} + (1 - \emptyset)\rho_{solution} \quad (10)$$

$$\mu_{nano} = \mu_{solution}(1 - 0.19\emptyset + 306\emptyset^2) \quad (11)$$

$$Cp_{nano} = (\emptyset\rho_{particle}Cp_{particle} + (1 - \emptyset)\rho_{solution}Cp_{solution})/\rho_{nano} \quad (12)$$

$$k_{nano} = [(k_{particle} + 2k_{solution} + 2(k_{particle} - k_{solution})(1 - 0.1)^3\emptyset)/[k_{particle} + 2k_{solution}(k_{particle} - k_{solution})(1 + 0.1)^2\emptyset)]\, k_{solution} \quad (13)$$

$$\alpha_{nano} = \frac{k_{nano}}{\rho_{nano}Cp_{nano}} \quad (14)$$

$$\vartheta_{nano} = \frac{\rho_{nano}}{\mu_{nano}} \quad (15)$$

$$Pr_{nano} = \frac{\alpha_{nano}}{\vartheta_{nano}} \quad (16)$$

at where $\emptyset$ is the volume fraction. The Reynolds number associated with the flow are obtained by:

$$Re_{nano} = \left[4\left(\frac{m_{nano}}{N_{tubes}}\right)\right]/(\pi D_{hnano}\mu_{nano}) \quad (17)$$

at where

$$D_{hnano} = 3.73\,10^{-3} \quad (18)$$

For turbulent flow if the thermal flow is completely developed, we have, approximately:

$$Nu_{nano} = 0,021\, Re_{nano}{}^{0,8} Pr_{nano}{}^{0,5} \quad (19)$$

For laminar flow regime in the water-base nanofluid, we have Nogueira [16], for the thermal input region under development:

$$Nu_{nano} = 1.409019812d0Z_{nano}{}^{(-0.3511653489)} \;;\; 10^{-5} \leq Z_{nano} < 10^{-3} \quad (20.1)$$

$$Nu_{nano} = 1.519296981d0Z_{nano}{}^{(-0.3395483303d0)} \;;\; 10^{-3} \leq Z_{nano} < 10^{-2} \quad (20.2)$$

$$Nu_{nano} = 10.8655 - 570.4671787Z_{nano} + 28981.67578Z_{nano}{}^2 - 950933.9838Z_{nano}{}^3 + 20237498.47Z_{nano}^4 - 276705269.6Z_{nano}{}^5 + 2340349265Z_{nano}{}^6 - 1.112482493^{10}Z_{nano}{}^7 + 2.269345238^{10}Z_{nano}{}^8 \;;\; 10^{-2} \leq Z_{nano} \leq 10^{-1} \quad (20.3)$$

$$Nu_{nano} = 5.261d0 - 19.93019048nano + 139.4921627Z_{nano}{}^2 - 605.9954034Z_{nano}{}^3 + 1716.100694Z_{nano}^4 - 3217.96875Z_{nano}{}^5 + 3954.86111Z_{nano}{}^6 - 3056.051587Z_{nano}{}^7 + 1344.246031nano^8 - 256.2830687Z_{nano}{}^9 \;;\; 10^{-1} \leq Z_w \leq 10^0 \quad (20.4)$$

Then, we have:

$$h_{nano} = h_w = Nu_{nano}\frac{k_{nano}}{D_{hnano}} \quad (21)$$

The heat transfer coefficients, h_a, and h_w are needed to obtain the overall heat transfer coefficient. Then, we have, for the air:

$$G_a = \frac{m_a}{A_{mín}} = \frac{m_a}{\sigma_a A_{fr}} \quad (22)$$

$$Re_a = \frac{G_a D_{ha}}{\mu_a} \quad (23)$$

$$J_{Lp} = \frac{h_a}{G_a c_{pa}} Pr_a{}^{2/3} \quad (24)$$

then,

$$h_a = J_{Lp}\frac{G_a c_{pa}}{Pr_a{}^{2/3}} \quad (25)$$

To determine the efficiency of the fin system, for the air heat exchange area, we have:

$$\eta = \frac{tgh(mL)}{mL} \quad (26)$$

at where

$$mL = \sqrt{2h_a/k_a t} \quad (27)$$

The efficiency weighted by the area is determined by:

$$\eta' = \beta\eta + 1 - \beta \quad (28)$$

at where

$$\beta = \frac{Fin\ area}{total\ area} \quad (29)$$

Then, we have:

$$\frac{1}{U_a} = \frac{1}{\eta' h_a} + \frac{1.0}{A_{med} K_{aleta}} + \frac{1}{(A_w/A_a) h_{nano}} \quad (30)$$

at where

$$A_{med} = \frac{A_a + A_{nano}}{2.0} \quad (31)$$

and

$$\frac{A_w}{A_a} = \frac{nanofluid\ side\ heat\ transfer\ area}{air\ side\ heat\ transfer\ area} \quad (32)$$

The number of thermal units, NTU, is obtained by the effectiveness theory:

$$NTU = \frac{A_a U_a}{C_{min}} \quad (33)$$

The thermal capacities are calculated by:

$$Ca = m_a * Cp_a \quad (34)$$

and

$$Cnano = m_{nano} * Cp_{nano} \quad (35)$$

Cmin is the lowest value between the thermal capacities of ethylene glycol and air. Finally,

$$Q = \varepsilon C_{min} \left(T_{h,af} - T_{c,af}\right) \quad (36)$$

at where

$$\varepsilon = 1 - exp\left[\frac{\left(\frac{c_{min}}{c_{max}}\right)^{-1} (NTU)^{0,22}}{\left\{exp\left[-\frac{c_{min}}{c_{max}} (NTU)^{0,78}\right] - 1\right\}}\right] \quad (37)$$

according to Kakaç [17].

The air and water exit temperatures are obtained through the energy balance equations:

$$Q = m_a c_{pa} \left(T_{a,af} - T_{a,ef}\right) \quad (38)$$

And

$$Q = m_{nano} c_{pnano} \left(T_{nano,ef} - T_{nano,af}\right) \quad (39)$$

In *Figure 1* below, we present the basic flowchart for the calculation process described above.

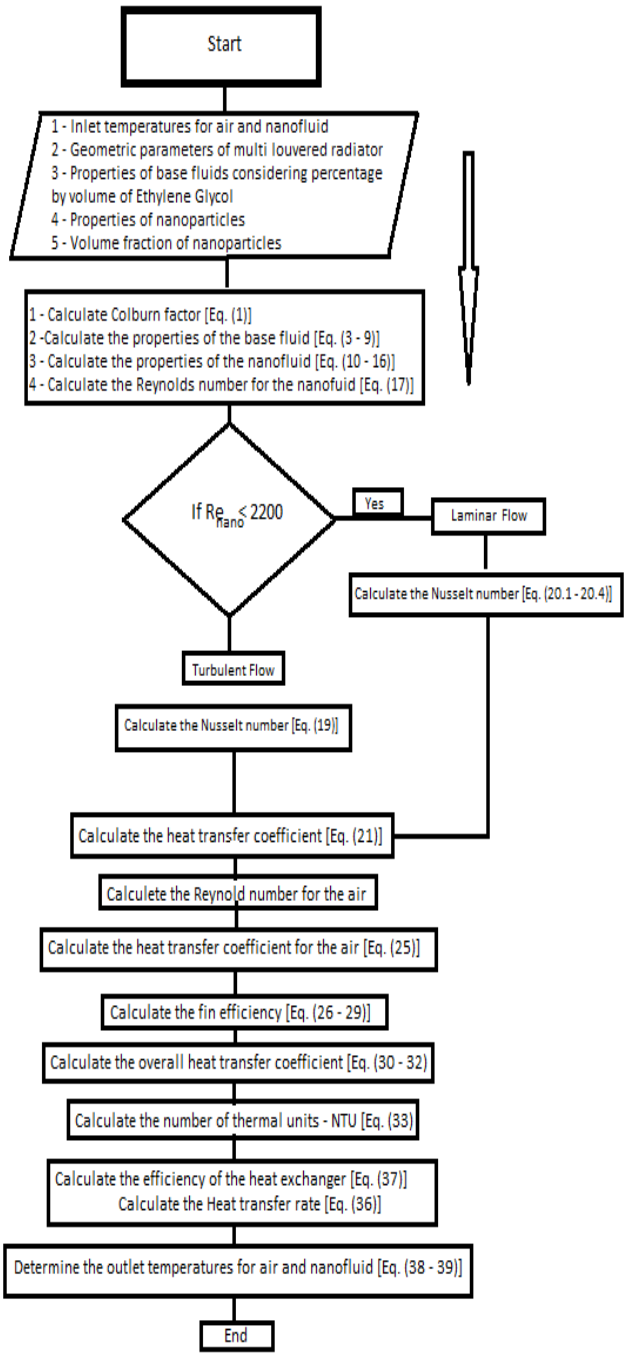

Figure 1 Basic flowchart for the calculation process

3.Results and discussion

Table 1 shows the numerical values of the necessary quantities, Equation 1, to obtain the Colburn Factor, which is represented graphically through *Figure 2*. The coefficient of heat transfer by convection in the air, ha, is described in *Figure 3*.

In *Figure 4*, we have the number of Reynolds as a function of the mass flow of the. An important aspect to be highlighted through the represented data is that the flow is laminar, for the whole range of mass flow considered when the volume fraction is significantly high.

Through *Figure 5*, the aspect verified through *Figure 4* is more evident, since, for the entire nanofluid flow range considered in the analysis, the Reynolds number is less than 2100 for relatively high nanoparticle fractions. For m_w = 2.0 Kg / s, the flow is laminar for all fraction of volume considered.

Table 1 Specification of the cross-section of Multi-Louvered fin parameters for the Colburn factor

Description	Fin dimension
Louver angle (L_a)	28
Fin pitch (F_p)	2 mm
Louver pitch (L_p)	1.2 mm
Fin height (F_h)	8 mm
Louver height (L_h)	6.5 mm
Louver length (L_d)	36.6 mm

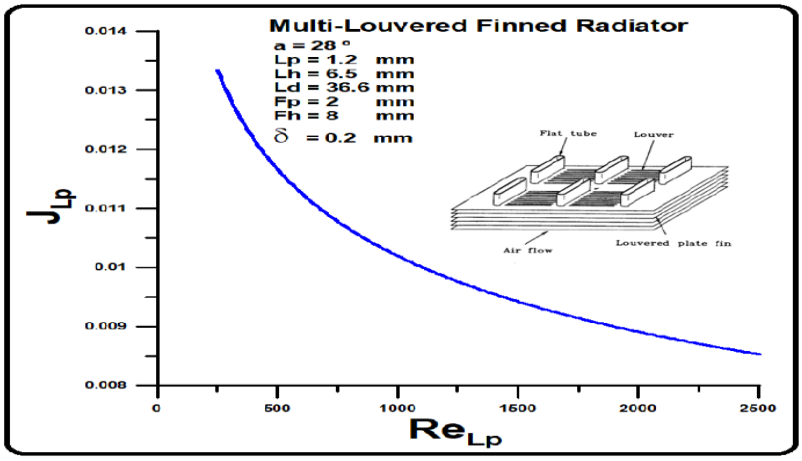

Figure 2 Fator de Colburn versus número de Reynolds

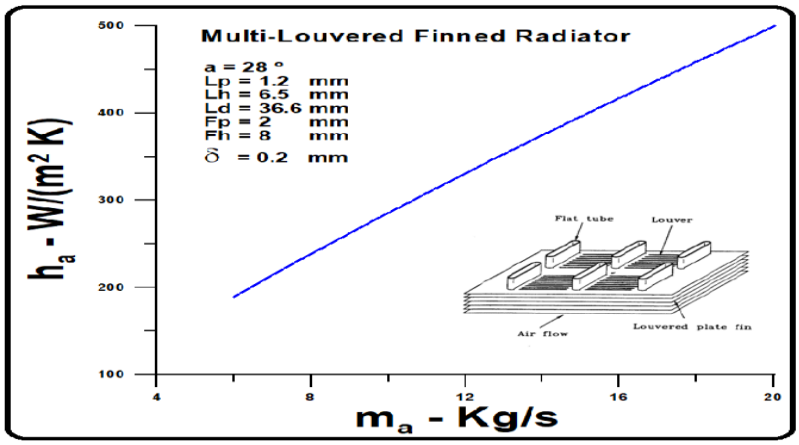

Figure 3 Convection heat transfer coefficient vs. mass air flow rate

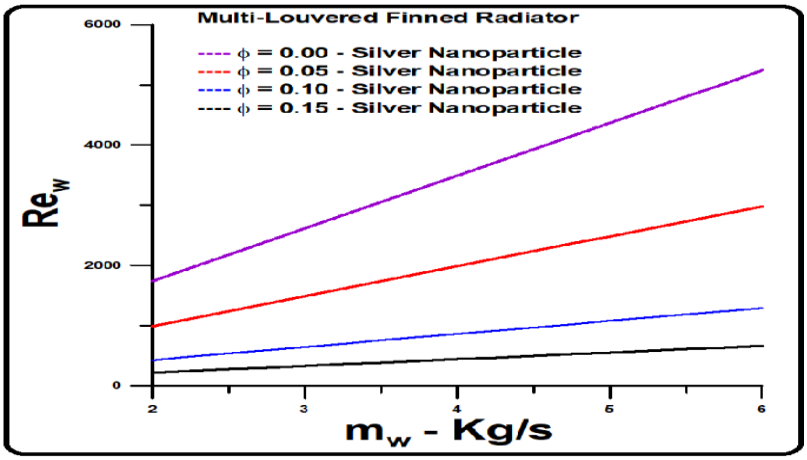

Figure 4 Reynolds number versus mass flow rate of the Nano fluid

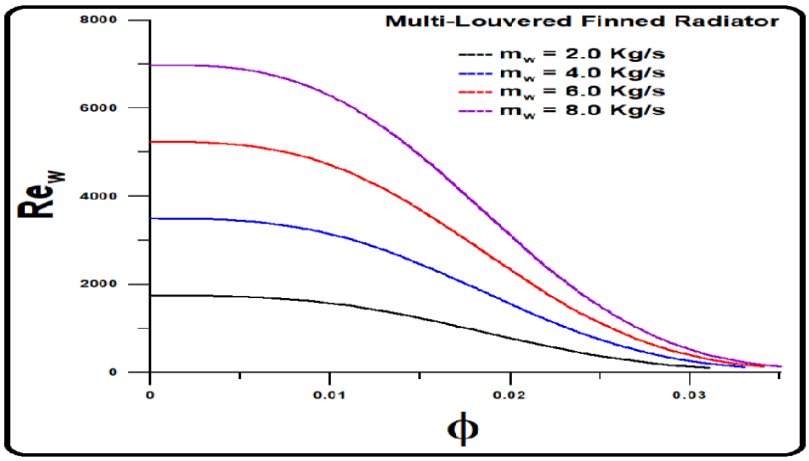

Figure 5 Reynolds number versus volume fraction of silver nanoparticles

The volume fraction needed for the flow rate to become laminar is a function of the mass flow rate of the nanofluid: for higher flow rates, more significant volume fractions.

Figure 6 shows the relationship between the convection coefficient of the nanofluid and the volume fraction of silver nanoparticles. For low nanofluid flow, mw = 2.0 Kg / s, where the flow is laminar for the entire range of volume fraction, the observed function is always increasing and smooth.
For a higher flow rate of nanofluid, it can be observed that the transition from turbulent to laminar flow occurs, as the volume fraction is increased. The transition for turbulent flow, as previously noted, occurs for progressively higher volume fraction values as the mass flow rate of the nanofluid increases.

The heat transfer coefficient of the nanofluid shows no difference between the flows, graphically observable, when the flow is laminar, for the entire flow range of the nanofluid.
The heat transfer rate with the mass flow of the nanofluid as a parameter is represented in *Figure 7*. High flow rates for the nanofluid, for a significantly low volume fraction, transfer higher energy in the form of heat for airflow rates below 12 kg / s of air.

Figure 5 shows the variation in the convection heat transfer coefficient versus mass flow rate of nanofluid, with volume fraction as a parameter. For high volume fractions, the heat transfer coefficient is relatively low, since the flow is laminar for the entire mass flow range considered. For small volume fractions, the heat transfer coefficient goes through the transition from laminar to turbulent flow. The convection heat transfer coefficient increases progressively, reaching relatively high values for a high mass flow rate, where the flow is turbulent.

The heat transfer rate as a function of the volume fraction of nanoparticles, with a mass flow rate of the fluid as a parameter, is represented by *Figure 6*. The volume fraction is constant and equal to 0.008. An extremely relevant fact, and worthy of note, is that for relatively low mass flow rates of the nanofluid, high heat transfer rates are possible for high mass airflow rates. As the coefficients of heat transfer from the air and nanofluid show increasing variation for mass flow rates, *Figures 4* and 8, the justification for higher heat transfer rates for low flow rates of the nanofluid, and high airflow rates, should be attributed to the high diffusivity of the nanofluid. At lower flow rates of the nanofluid, it is expected that the diffusivity has greater relevance.

The heat transfer rate is represented by *Figure 7* as a function of the airflow rate, with the nanofluid flow rate as a parameter. For relatively low airflow rate values, the heat transfer rate increases with the increase in the mass flow rate of the nanofluid. It is demonstrating that for low airflow rate, the heat transfer exchange effect on the nanofluid surface is predominant when the flow in the tube is turbulent. For high airflow rates, the exchange rate is higher for lower nanofluid flow rates, demonstrating that for low nanofluid flow rates, the most considerable heat exchange occurs due to the finned radiator geometry. A significant fact is that the heat transfer rate for high flow rates of nanofluid is not affected by the volume fraction of the nanoparticles, to any extent analyzed for airflow rate.

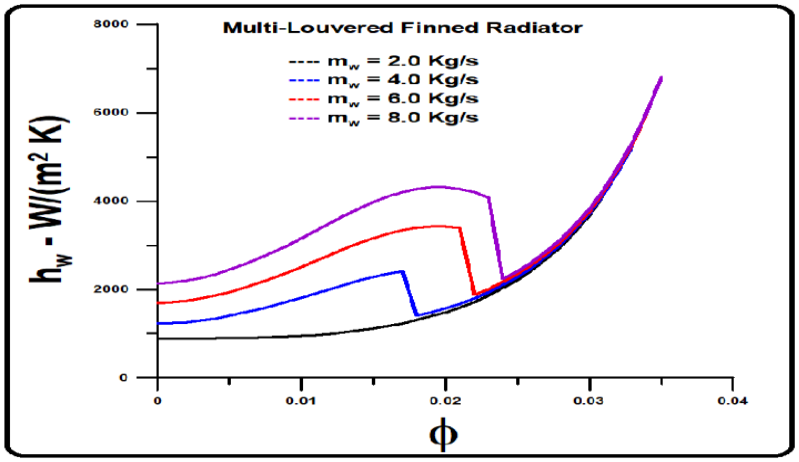

Figure 6 Convection heat transfer coefficient in Nano fluid versus volume fraction of silver Nanoparticles

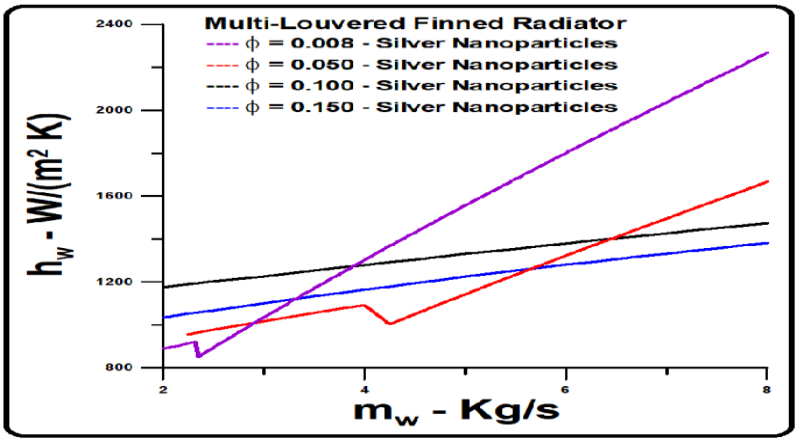

Figure 7 Convection heat transfer coefficient versus mass flow rate of the Nano fluid

The outlet temperature of the nanofluid is represented in *Figure 8*. The temperature of the entrance of the nanofluid, for all situations considered in the analysis, is equal to 100 ºC. The best performance, with lower outlet temperatures, is for relatively lower flow rates of the nanofluid. This result is due to the more considerable influence of nanofluid diffusivity for low flow rates.

The difference in outlet temperature for pure ethylene glycol, with the outlet temperature of the relatively high-volume fraction of the nanofluid, is significant for the low flow of nanofluid, m_w = 2.0 Kg / s. This difference in outlet temperature tends to decrease for higher flow rates of the nanofluid, that is, for extremely high flow rates of the nanofluid, there is no justification for adding silver nanoparticles.

The air inlet temperature is equal to 30 ºC for all situations analyzed. The air outlet temperature, *Figure 9*, presents results compatible with those observed in *Figure 8*. That is, for extremely high flow rates of the nanofluid, there is no justification for adding silver nanoparticles. *Figure 10* shows the thermal efficiency of the radiator considered for analysis, with a volume fraction of the nanoparticles as a parameter and mass flow rate of the fixed nanofluid. The highest efficiency occurs in a low volume fraction of the nanoparticles and low mass flow of air.

Figure 11 shows the efficiency of the radiator. It can be seen that there is a qualitative equivalence with the results presented in *Figure 9* since there is a low efficiency when the flow rate in the volume of the nanofluid is low, and the airflow is low. However, efficiency is relatively high for low nanofluid flow rates and high airflow rates. For high flow rates of the nanofluid, the efficiency decreases with the airflow variation and has high efficiency for low airflow rates. However, there is no justification for the inclusion of nanoparticles in the latter case since the efficiency is practically equal to that of pure Ethylene Glycol.

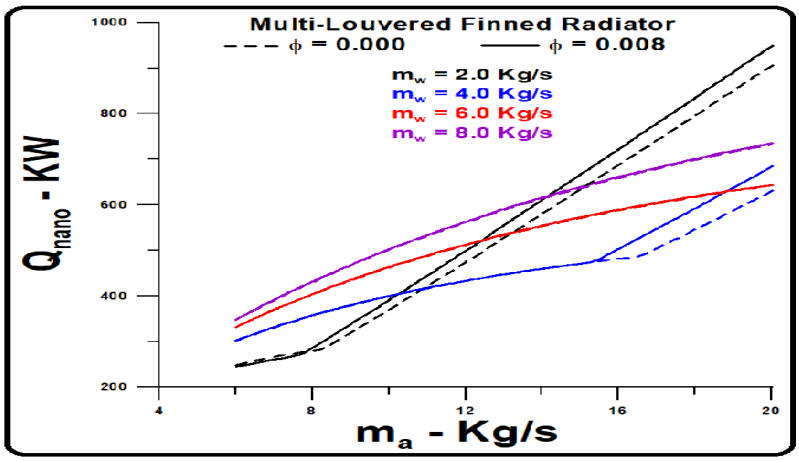

Figure 8 Heat transfer versus mass air flow rate

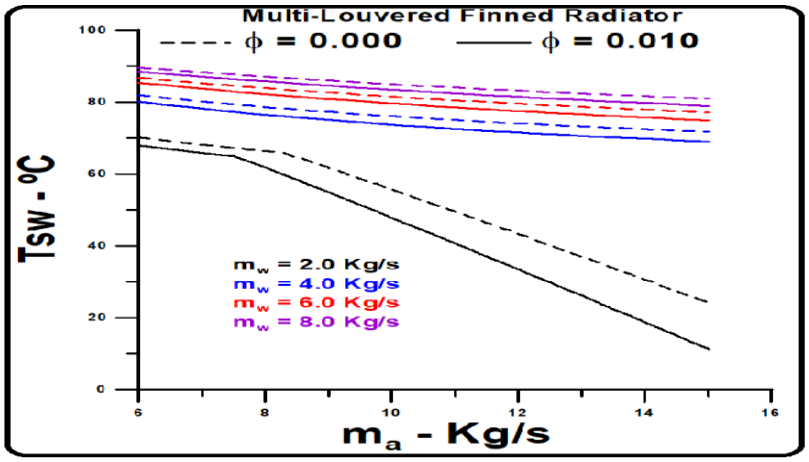

Figure 9 Output temperature of the Nano fluid as a function of the mass flow of the air

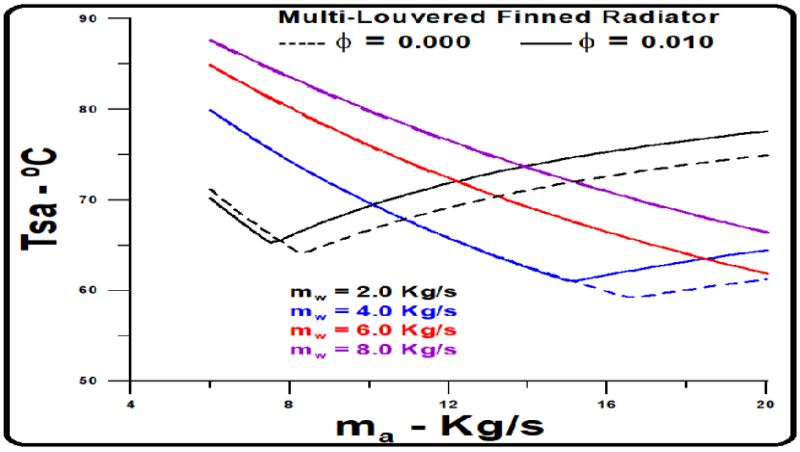

Figure 10 Temperatura de saída do ar em função da vazão em massa do ar

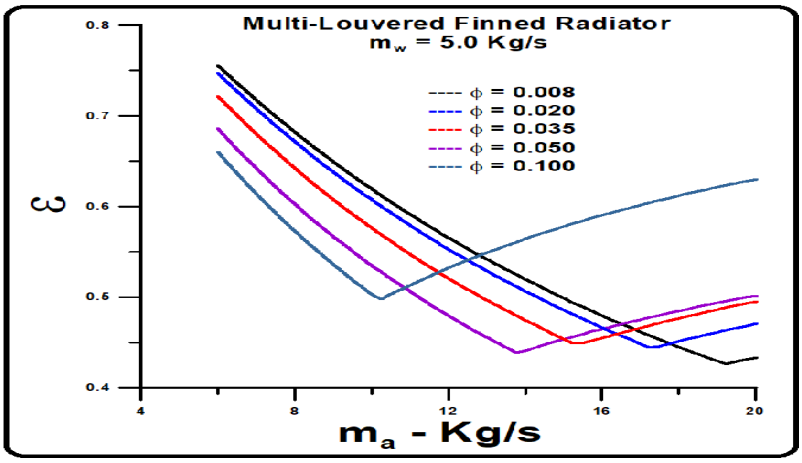

Figure 11 Radiator efficiency as a function of the mass flow of air, with volume fraction as a parameter

The diffusion process in the nanofluid is the main responsible for the high efficiency in low airflow and low values, as shown in *Figure 12*. However, as the volume fraction of the nanoparticles increases, the efficiency decreases, to a point where the heat exchange by the fins becomes the main factor responsible for the heat exchange. For high air flow rates and high-volume fractions of the nanoparticles, the efficiency approaches the unit but is significantly low for low volume fraction values.

Due to the observations made above, concerning the data presented, it is evident that the radiator in question shows excellent performance for low volume fraction values of silver nanoparticles, low airflow rates, and low nanofluid rates. A promising result, as it can save on the use of the compact heat exchanger, reducing costs and storage space for the refrigerant (*Figure 13*). However, excellent thermal performance can be achieved for high volume fractions of silver nanoparticles and high airflow rates. As demonstrated, the thermal performance for high nanoparticle fractions is equivalent to the pure Ethylene Glycol. In the latter case, the fin system used prevails in the heat exchange, to the detriment of the heat exchange that occurs in the nanofluid.

Although the theoretical approach presented is based on concepts and procedures already proven by countless studies presented in the literature of compact heat exchangers [18─20], an experimental evaluation of the heat exchanger in question would be extremely relevant.

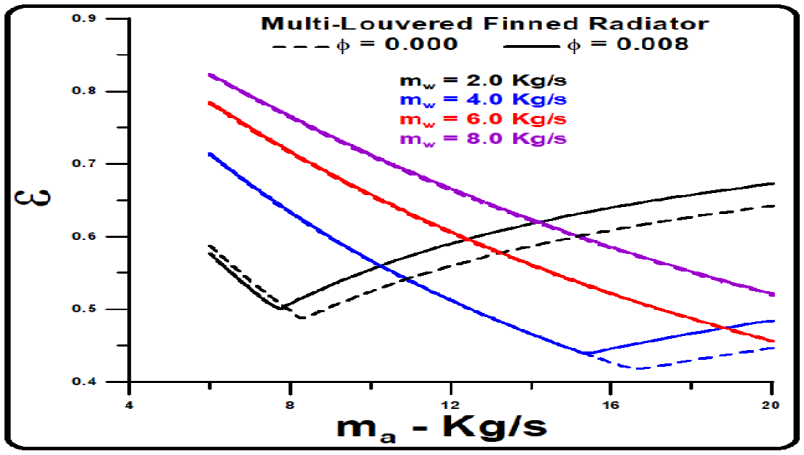

Figure 12 Radiator efficiency as a function of mass airflow, with the nanofluid flow as a parameter

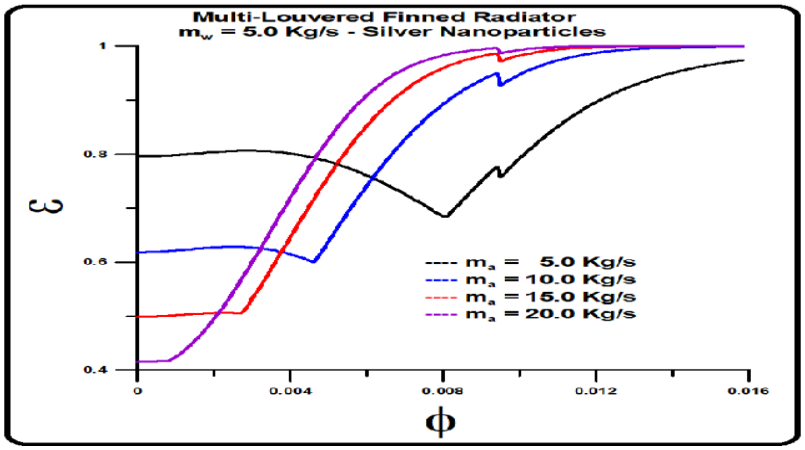

Figure 13 Radiator efficiency as a function of volume fraction, with airflow as a parameter

4.Conclusions

The best performance is obtained for a relatively low fraction of silver nanoparticles when the turbulent effect is high, and the greater diffusivity of the base fluid becomes more effective.

As demonstrated, the thermal performance for high nanoparticle fractions is equivalent to the performance of pure ethylene glycol. In these situations, the fin system used to prevail in the heat exchange, to the detriment of the heat exchange that occurs in the Nano fluid. For a high fraction of nanoparticles, it is expected that the applied methodology does not work correctly, because the flow is no longer Newtonian.

Acknowledgment

None.

Conflicts of interest

The authors have no conflicts of interest to declare.

References

[1] Yadav JP, Singh BR. Study on performance evaluation of automotive radiator. S-JPSET. 2011;2(2):47-56.

[2] Sany AE, Saidi MH, Neyestani J. Experimental prediction of nusselt number and coolant heat transfer coefficient in compact heat exchanger performed with E-NTU method. The Journal of Engine Research. 2010; 18:62-70.

[3] Yerrennagoudaru H, Manjunatha K, Prasad BV, Sandeep K, Kumar SV. International Journal of Engineering Science and Innovative Technology. 2016;5(4):82-9.

[4] Jing H, Quan Z, Zhao Y, Wang L, Ren R, Liu Z. Thermal performance and energy saving analysis of indoor air–water heat exchanger based on micro heat pipe array for data center. Energies. 2020; 13(2):1-24.

[5] Blecich P, Trp A, LENIÆ K. Calculation method for fin-and-tube heat exchangers operating with nonuniform airflow. WIT Transactions on Ecology and the Environment. 2019; 237:13-24.

[6] Hussein AM, Bakar RA, Kadirgama K, Sharma KV. Heat transfer enhancement using nanofluids in an automotive cooling system. International Communications in Heat and Mass Transfer. 2014; 53:195-202.
[7] Kim NH, Cho H. Airside heat transfer and pressure drop of louver-finned parallel flow heat exchanger having a drainage channel. Journal of Thermal Science and Technology. 2018;13(1):1-14.
[8] Pankaj RB, Rangarajan S, Nagaraja SR. Analytical performance analysis of cross flow louvered fin automobile radiator. In MATEC web of conferences 2018 (p. 02003). EDP Sciences.
[9] Gomaa ME. Experimental and numerical investigations on the automotive radiator performance using louvered-fin heat exchanger. Journal of Engineering Sciences.2009; 37(2):345-62.
[10] Dong J, Chen J, Chen Z, Zhang W, Zhou Y. Heat transfer and pressure drop correlations for the multi-louvered fin compact heat exchangers. Energy Conversion and Management. 2007; 48(5):1506-15.
[11] Sarkar J, Tarodiya R. Performance analysis of louvered fin tube automotive radiator using nanofluids as coolants. International Journal of Nanomanufacturing. 2013; 9(1):51-65.
[12] Nogueira E. Thermal-hydraulic performance of graphene nanoribbon and silicon carbide nanoparticles in the multi-louvered radiator for cooling diesel engine. Journal of Engineering Sciences. 2020.
[13] Dwivedi VD, Rai R. Design and performance analysis of louvered fin automotive radiator using CAE Tools. International Journal of Engineering Research & Technology. 2015; 4(1):30-4.
[14] Junior LC, Nogueira É. Influence of the coolant flow containing silver nanoparticles (ag) from an aqueous solution based on ethylene glycol (EG50%) on the thermal-hydraulic performance of an automotive radiator. World Journal of Nano Science and Engineering. 2020; 10(01).
[15] Nogueira É. Thermal performance of ethylene-based aqueous solutions containing silver (Ag), Copper Oxide (CuO), Aluminum Oxide (Al2O3) or Titanium Dioxide (TiO2) nanoparticles in a finned flat tube compact heat exchanger (Automotive Radiator). The International Journal of Engineering and Science. 2019; 7:56-9.
[16] Nogueira E. Laminar flow and heat transfer in immiscible fluids without stratification. Technological Institute of Aeronautics. 1988.
[17] Kakaç S. Boilers, evaporators, and condensers. John Wiley & Sons; 1991.
[18] Silaipillayarputhur K, Khurshid H. The design of shell and tube heat exchangers–a review. International Journal of Mechanical and Production Engineering Research and Development. 2019; 9(1):87-102.
[19] Arvind RD. Heat transfer analysis of shell and tube heat exchanger using aluminium nitride-water nanofluid. International Journal on Applications in Mechanical and Production Engineering. 2015; 1(1):13-5.
[20] Kumar N, Sonawane SS. Convective heat transfer of metal oxide-based nanofluids in a shell and tube heat exchanger. In conference proceedings of the second international conference on recent advances in bioenergy research 2018 (pp. 183-92). Springer, Singapore.

Élcio Nogueira Was born in Muzambinho, Minas Gerais, Brazil, in 1954. Ph.D. in Mechanical Engineering from the Federal University of Rio de Janeiro - UFRJ / COPPE (1993) and Post-Doctorate in Thermal Sciences at the University of Miami - USA (1995). Master in Aeronautical and Mechanical Engineering by Technological Institute of Aeronautics - ITA (1988). Specialization in Thermal Sciences from the Federal University of Viçosa - UFV (1985). Specialization in Leadership and Educational Management by Iberoamerican University Organization – OUI (2000), with internships in Argentina and Mexico. Holds a degree in Physics from the Federal University of São Carlos with Extension in Nuclear Engineering – UFSCar (1981). Adjunct Professor, Faculty of Technology, State University of Rio de Janeiro - FAT / UERJ. Research topics: Transport Phenomena, Mathematical and Computational Methods, Two-Phase Flow, Applications of Nanofluids, Hypersonic Flow, Boundary Layer with the application of Similarity Method.
Email: elcionogueira@hotmail.com